International Transaction Journal of Engineering, Management, & Applied Sciences & Technologies

http://TuEngr.com

PAPER ID: 11A03F

BEHAVIORAL SIMULATION OF INDUCTION MOTOR TEMPERATURE DISTRIBUTION

Alexander A. Pugachev [a*], A.Yu. Drakin [a], A.N. Shkolin [a]

[a] *Department of Industrial Electronics and Electrical Engineering, Bryansk State Technical University, RUSSIA.*

ARTICLEINFO

Article history:
Received 01 July 2019
Received in revised form 18 October 2019
Accepted 31 October 2019
Available online 26 November 2019

Keywords:
Asynchronous motor; AC electric motor; Behavioral simulation; Equivalent thermal circuit; Power losses; Finite element model; Differential equations; Control system; State and rotor windings; Cooling system; Overheating.

ABSTRACT

The paper justifies the need to monitor and control the thermal state of the induction motor as a whole and its windings, as the most heat-loaded elements. A review of modern methods of measuring and determining the temperature of windings (including rotating) is carried out. It showed trends in the use of non-contact methods for determining temperature using mathematical models based on the finite element method and relevant thermal equivalent circuits. To determine the temperature distribution, an equivalent thermal model of an induction motor, consisting of 53 nodes, 31 of which are heat generating was developed. To determine the losses, a T-shaped equivalent circuit for replacing motor windings was used, taking into account losses in steel, non-linearity of the magnetization curve and the effect of current displacement in the rotor winding. The simulation results in steady and transient modes are presented.

Disciplinary: Electrical Engineering (Motor Engineering).

1. INTRODUCTION

The widespread use of induction machines in industry and transport is explained by a number of circumstances (Krishnan, 2001; Novotny & Lipo, 1996; Kosmodamianskii et al., 2012):

- the mass of a squirrel-cage induction motor is 1.5-2 times less than the mass of a DC motor of the same power;

- the torque of inertia of the rotor of a short-circuited traction induction motor is two times greater than that of a DC motor;

- the cost of a squirrel-cage induction motor is about 2-3 times less than the cost of a DC motor.

In recent years, significant efforts have been directed towards the development of methods for diagnosing damage and malfunctions of induction machines, as well as the creation of methods for their protection. The most important part of any protection is the availability of thermal protection,

*Corresponding author (A.A.Pugachev) Email: alexander-pugachev@rambler.ru

which is necessary to eliminate thermal overloads, and, therefore, extend the traction motor life. Thermal overloads that cause motor damage lead to much more intense insulation damage. In addition, they can lead to failure of the key elements of the machine: insulation of the stator windings, rotor rods, stator core, and rotor, etc.

In Motor Reliability Working Group (1985), an investigation of the damage causes and the analysis of components that fail during the induction motor operation is given. The main results of this work are summarized in Table 1.

Table 1: Damages during the induction motor operation.

Causes of damage	**%**	**Damaged unit**	**%**	**On average**
Constant overloads	4,2	Stator housing insulation	23	Damage caused by electrical reasons *33,3 %*
Insulation aging	26,4	Winding insulation	4	
		Wiring clamp	3	
		Stator core	1	
		Stems of the "squirrel" cage	5	
Total	*30,6*	*Total*	*36*	
Increased vibration	15,5	Plain bearing	29	
Deteriorated lubrication	15,2	Rotor shaft	2	Damage caused by Mechanical reasons *31,35 %*
		Rotor core	1	
Total	*30,7*	*Total*	*32*	
High ambient temperature	3	Bearing seats	6	Damage caused by operating conditions and other reasons *35,35 %*
Humidity changes	5,8	Oil (grease) leak	3	
Voltage imbalance	2,1	Frame	1	
Chemically hazardous environment	4,2	Cooling fins	1	
Poor cooling	3,9			
Other reasons	19,7	Other units	21	
Total	*38,7*	*Total*	*32*	

Despite different evaluation criteria, both studies show a very close percentage of damage caused by electrical and mechanical reasons.

Analyzing the data shown in Table 1, a larger number of damage is caused by the heating of certain parts of the electric machine.

Overheating of the insulation of the motor windings is usually caused by the following reasons:

- dynamic overloads during transients (starting, braking, reverse, switching to another speed);
- high mechanical loads, and, as a result, high currents in the windings (thermal overloads);
- an asymmetric source of electricity;
- high ambient temperature;
- poor cooling conditions.

It was shown in (Kosmodamianskii et al., 2011), that the frontal part of the most loaded stator phase experiences the greatest thermal loads with asymmetries in the supply voltage. According to the studies conducted for the most unfavorable phase shift value, with asymmetry coefficient values of up to 2% and direct sequence voltage drops of up to 5%, thermal overloads can reach 10 ... 17%, resulting in a significant reduction in the period of trouble-free operation.

Kosmodamianskii et al. (2011) studied the effects of temperature on the static mechanical characteristics of an electric drive with an ED-900 induction motor, see results in Figure 1.

A general view of the mechanical characteristics is shown in Figure 1, a (designations: *M* - motor torque, *w* - rotor speed). An analysis of the graphs (Figure 1) allows us to conclude that an increase in

the temperature of the windings θ of the induction motor entails a decrease in the critical torque *Mm* (Figure 1, b) and an increase in the absolute critical slip *sk* (Figure 1(c)), which causes a significant decrease in the stiffness of the mechanical characteristics of β (Figure 1(d)).

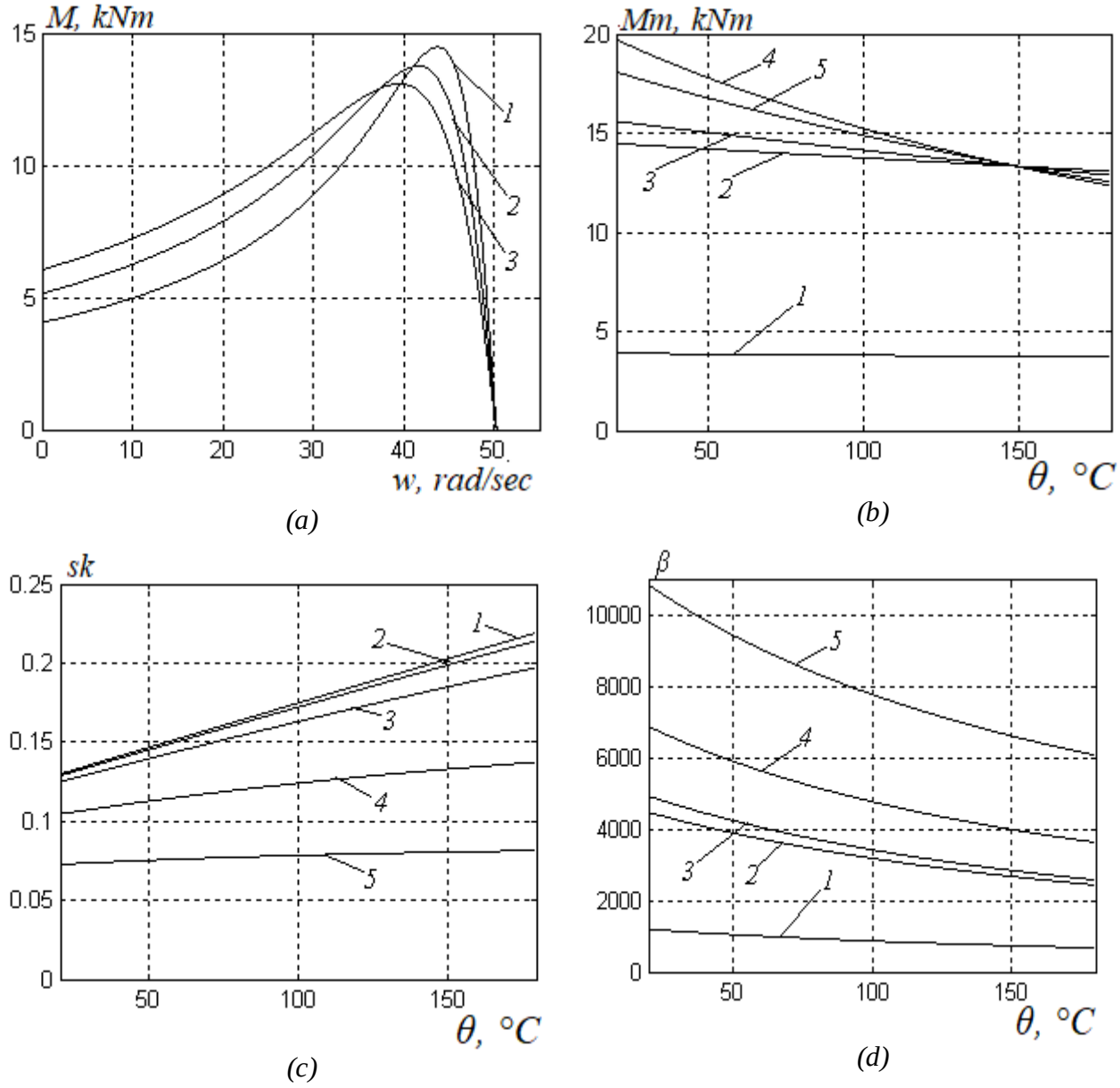

Figure 1: Mechanical characteristics (a) at nominal parameters of the supply voltage (*1– θ = 20°C, 2– θ = 100°C, 3– θ = 180°C*), dependences of the critical torque (b), absolute critical slip (c) and stiffness (d) on the temperature of the windings (*1 – f_1 = 48 Hz, 2 – f_1 = 24 Hz, 3 – f_1 = 12 Hz, 4 – f_1 = 4.8 Hz, 5 – f_1 = 2.4 Hz).*

This is explained by an increase in temperature with an increase in the active resistance of the stator and rotor windings, which leads to a decrease in the absolute critical slip, since the temperature dependence of the inductive resistance of the windings is weak, and the stator supply voltage does not affect the critical slip value at all. A change in the absolute critical slip under the influence of temperature is more pronounced in the zone of high frequencies of the stator current (42% at a stator current frequency of f_1 = *48 Hz*). The smallest slipe sensitivity to temperature is manifested at low frequencies (13% at a stator current frequency of f_1 = *2.4 Hz*) since in this mode it is determined mainly by the ratio of the active resistance of the stator and rotor windings.

The critical torque decreases significantly with increasing temperature, which is the most

*Corresponding author (A.A.Pugachev) Email: alexander-pugachev@rambler.ru Volume 11 No.3 ISSN 2228-9860 eISSN 1906-9642 CODEN: ITJEA8
Paper ID:11A03F http://TUENGR.COM/V11/11A03F.pdf DOI: 10.14456/ITJEMAST.2020.46

pronounced in the low-frequency zone (at a nominal frequency $f_1 = 24$ *Hz*, the decrease in torque is 10.5%, at the stator current frequency of 2.4 Hz - 55%). When operating at high frequencies (in the second zone), the influence of the temperature of the windings is weakly expressed, since the operation in this mode is determined mainly by the short circuit inductive resistance.

A similar effect of temperature on the torque and slip leads to a decrease in stiffness with increasing temperature, the more the lower the stator current frequency is (71% at a stator current frequency of $f_1 = 2.4$ *Hz*, 5% at a stator current frequency of $f_1 = 48$ *Hz*)

In (Lim & Nam, 2004), the economical coefficient is taken as a criterion for evaluating the electric drive efficiency:

$$\varepsilon(f_2) = \frac{I_1^2}{\mathrm{M}} \rightarrow min \qquad (1)$$

where I_1 – stator winding current;

M – torque developed by the electric drive.

Figure 2 shows the dependences of the coefficient $\varepsilon(f_2)$ for the DAT-305 motor.

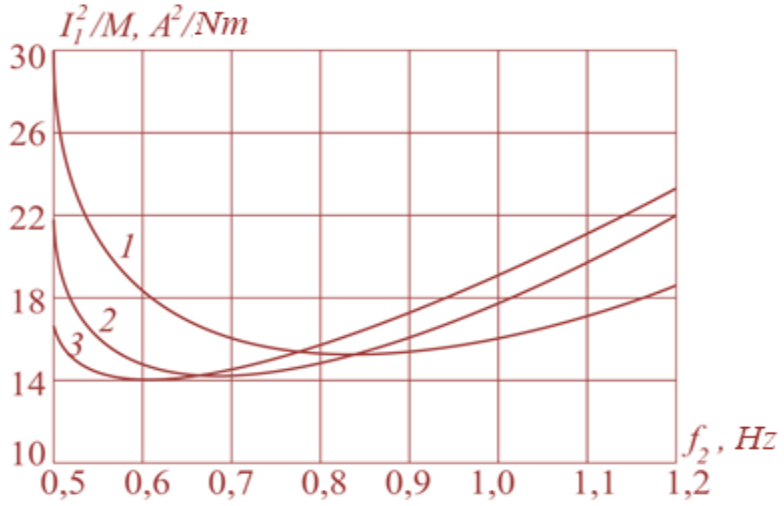

1 – θ = 165°C, 2 – θ = 130°C, 3 – θ = 95°C.

Figure 2: The dependence of the DAT-305 motor efficiency coefficient on the rotor current frequency f_2 at various values of the temperature of the windings θ

Figure 2 shows that when the temperature of the traction motor windings increases, the rational value of the rotor winding current, according to the condition $\varepsilon(f_2) \rightarrow min$, shifts to the large slip zone: at θ = 95 ºC, $f_{2\,opt}$ = 0.63 Hz, at θ = 165ºC, $f_{2\,opt}$ = 0.87 Hz. The stator current and voltage amplitudes themselves, delivering $\varepsilon(f_2) \rightarrow min$, vary insignificantly. The deviation of the rotor current frequency from the rational leads to a sharp increase in the stator winding current and an increase in the economic coefficient.

Despite the rational control of the motor running at all temperatures with the lowest possible stator current values, with an increase in the temperature of the windings, its efficiency coefficient decreases because the value of the efficiency coefficient ε (f2) increases: at the temperature of the windings θ = 0°C, $\varepsilon(f_2)$ = 10.5 A^2/Nm; at a temperature of the windings θ = 180°C, $\varepsilon(f_2)$ = 14.4 A^2/Nm.

An increase in losses with increasing temperature will inevitably lead to a decrease in traction motor efficiency: with an increase in temperature in the range of 0 ... 180°C, efficiency decreases from 89 to 77% (Kosmodamianskiy et al., 2015). At the same time, the torque on the shaft of the traction motor decreases.

Thus, in modern control systems, it is necessary to take into account the influence of the temperature of the windings on the processes occurring in the power and control systems (Kosmodamianskiy et al., 2015; Kosmodamianskii et al., 2015).

2. METHODS USED TO STUDY THE INDUCTION MOTOR THERMAL STATE

In the process of studying the thermal processes of motors, the following temperature control methods can be used: the resistance method, the method of built-in temperature sensors, and the thermometer method.

The resistance method involves the use of the dependence of the resistance of the motor windings on temperature. In this case, the average temperature of the motor winding is measured, both with the voltage removed and with the voltage applied. The main disadvantage of this method is the significant hardware costs in the case of motors operated under voltage.

A prerequisite for using the second method of built-in temperature sensors when determining the temperature of electric motor assemblies is the presence of built-in temperature sensors such as thermocouples, resistance thermometers, infrared temperature sensors, etc., for example, in the array of the motor stator winding. The implementation of this technical solution seems possible only in the manufacture of the motor. At the same time, only a small part of the motors operated today have such sensors in their design, which is explained by a number of economic and technical reasons related to the cost, difficulty of installing sensors and their operation.

Using the third method involves registering the motor surface temperature. The lack of information about the temperature of its internal nodes is the main disadvantage of this temperature control method.

Currently, taking into account the development of the microprocessor and digital systems, a method for controlling the induction motor temperature based on the data of a mathematical model of thermal processes calculated with the help of known (measured) electrical parameters as well as motor design parameters is widely used.

The choice of the thermal model should be based on a comprehensive analysis of the induction motor (IM) operating environment. In modern conditions, there is a need to develop thermal models to analyze the operation of induction electric drives with frequency control.

The mathematical modeling of thermal processes occurring in an electric motor has been the subject of many scientific works (Staton, 2001; Mahdavi et al., 2013; Kylander, 1995; Pugachev & Kosmodamianskii, 2017; Mellor et al., 1991; Staton & Cavagnino, 2008; Champenois et al., 1994; Huai et al., 2003; Trigeol et al., 2006; Mezani et al., 2005; Kosmodamianskii & Pugachev, 2018; Briz et al., 2008). Moreover, the methods discussed in them are divided into two types: using the finite element method (FEM) and using the equivalent thermal circuits (ETC).

The application of the FEM method involves a significant amount of calculations using special software systems, such as ANSYS, which makes it possible to simulate thermal fields, as well as the availability of obtaining detailed information about the geometric dimensions of the motor structural components. Staton (2001) considered the features of convective exchange between air flows in the motor cooling channels. The issues related to natural and forced cooling are analyzed. The relevant criteria and design relationships for determining the Nusselt number are given. Moreover, the calculations for stationary thermal processes were performed. In (Mahdavi et al., 2013), using FEM,

*Corresponding author (A.A.Pugachev) Email: alexander-pugachev@rambler.ru Volume 11 No.3 ISSN 2228-9860 eISSN 1906-9642 CODEN: ITJEA8
Paper ID:11A03F http://TUENGR.COM/V11/11A03F.pdf DOI: 10.14456/ITJEMAST.2020.46

modeling of non-stationary thermal processes occurring in the motor stator was made. According to the results of experimental studies, it was concluded that the mathematical model has high accuracy in the simulation of stationary thermal processes, and in dynamics, an error can reach 10°C.

The second type of methodology, based on ETC, is widely used in the development and study of motors. It allows determining the average temperature values of individual motor nodes.

There is a fairly large number of scientific works devoted to the study of the induction motor thermal state based on ETC (Kylander, 1995; Pugachev & Kosmodamianskii, 2017; Mellor et al., 1991). In all of them, schemes with varying degrees of detail, with a different number of nodes and heat-loaded nodes of the induction motor are used. However, in most works there are no calculation formulas and calculation methods for determining the thermal resistances of these equivalent circuits are not given. Along with this, a correct determination of the thermal model resistances is the key to its adequate operation in steady and transient modes.

To numerically solve the problem of inhomogeneous heat conduction in a body with distributed heat sources, the finite difference method is used, which, with a grid step commensurate with the linear dimensions of the IM elementary nodes, is converted to the method of equivalent thermal circuits (ETC) for solving three-dimensional problems of heat conduction and heat transfer.

When using the ETC method to calculate temperature fields in an electric machine, a heat system with continuously distributed parameters is replaced by an equivalent system of homogeneous bodies (nodes), between which conductive connections, determined by the corresponding heat exchange processes are established, which allows such systems of equations to be solved by standard numerical methods.

The basis for such a transition is the ability to consider the distribution of the thermal field in the element as a result of the interaction of several one-dimensional heat fluxes. The error that arises, in this case, depends on the linear dimensions of the elementary nodes.

When calculating the temperature fields of electric machines for research purposes, the number of nodes the machine is divided into can be selected by almost anyone that guarantees a given calculation accuracy. For circuit nodes with insignificant heat reduced capacity in comparison with other nodes, namely, for the nodes of the air flows in the machine channels, on the basis of the theory of heat transfer in thermally coupled bodies, the differential equations describing the thermal state of the nodes are replaced by algebraic equations.

The general form of the equation describing the thermal state of the *i-th* node of the system that is in contact with adjacent *n* nodes has the form

$$\frac{\P q_i}{\P t} = P_i - \sum_{n=1}^{n} \frac{q_i - q_n}{R_{i,n}}, \qquad i = 1...n. \tag{2}$$

$\P q_i$ – a small increment of the temperature of the *i-th* node, ° C for a small-time increment $\P t$, c;

P_i – the power loss of the *i-th* node, W (equal to zero if the node is passive);

q_i – instant value of the temperature of the *i-th* node, °C;

q_n – the instantaneous temperature of the adjacent node, °C (1 ... n);

$R_{i,n}$ – the thermal resistance of an adjacent node (1 ... n) in contact with the *i-th* node, °C/W;

$\sum_{n=1}^{n} \frac{q_i - q_n}{R_{i,n}}$ – the sum of the differences in the instantaneous temperatures of the *i-th* node with

each contacting adjacent node (1 ... n), assigned respectively to the thermal resistances of these nodes, W.

The ETC method, as it was said above, consists in determining the average temperatures of individual motor nodes. It can be used not only to study the stationary thermal state of the motor but also in the case of unsteady thermal states.

The thermal state of the motor for non-stationary thermal conditions can be described by a complex system of interconnected elements. The processes taking place in these elements can be represented by a system of differential equations in partial derivatives with interconnected boundary conditions.

If we make an assumption (not considering the temperature fields of each individual motor node), then we can use the first-order system of linear differential equations to describe the unsteady heat process. In this case, the number of equations is equal to the number of bodies the motor is divided into. In this case, the number of ETC nodes should equal the number of bodies. The differential heat balance equation is written for each ETC node.

Staton & Cavagnino (2008) indicated an increase in motor average temperature values up to 29%. Due to the fact that the additional losses in the rotor are about 65% of the total additional losses of the motor, the most significant is their combined influence along with changing cooling conditions. An analysis of the works related to the calculation and experimental studies of the thermal state of frequency control motors under various control laws makes it possible to conclude that the temperature distribution along the length of the rotor array has the form of an asymmetric bell.

Based on a review of literature (Staton, 2001; Mahdavi et al., 2013; Kylander, 1995; Pugachev & Kosmodamianskii, 2017; Mellor et al., 1991; Staton & Cavagnino, 2008; Champenois et al., 1994; Huai et al., 2003; Trigeol et al., 2006; Mezani et al., 2005; Kosmodamianskii & Pugachev, 2018; Briz et al., 2008)., the ETC method was adopted as the chosen method for studying the temperature distribution in the induction motor, which enables us to calculate the thermal state of motor components in all modes of its operation with a slight error.

3. EQUIVALENT THERMAL CIRCUIT OF THE INDUCTION MOTOR

The motor has a complex structure, which complicates the task of its thermal modeling. The complexity and at the same time the accuracy of the thermal model will largely depend on the number of nodes considered. Critical temperatures are recorded for various parts of the stator a rotor winding of induction motors. It is important to take this into account when developing an equivalent thermal model and design such motor units with a large number of elements to achieve the most accurate calculation results.

The general view of the IM ETC is schematically shown in Figure 3(a).

From the thermal point of view, the induction motor consists of fifty-three heat-loaded nodes, 31 of which are heat-generating ones (in Figure 3(b) the heat-generating (active) nodes are made with black filling (for example, unit 19), passive units have no filling). The selection of these nodes was made on the basis of a review of studies of the thermal state of induction motors of various designs, purposes, and cooling schemes.

A fragment of the designed ETC corresponding to the sketch is shown in Figure 3(b). ETC is symmetrical about the vertical axis and the right-hand side (is not shown in Figure 3(b)) is similar to

*Corresponding author (A.A.Pugachev) Email: alexander-pugachev@rambler.ru Volume 11 No.3 ISSN 2228-9860 eISSN 1906-9642 CODEN: ITJEA8
Paper ID:11A03F http://TUENGR.COM/V11/11A03F.pdf DOI: 10.14456/ITJEMAST.2020.46

the left-hand side (fragment is shown in Figure 3(b).

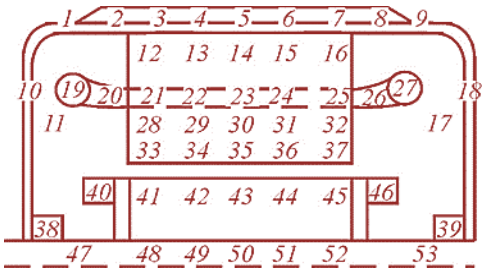

(a)

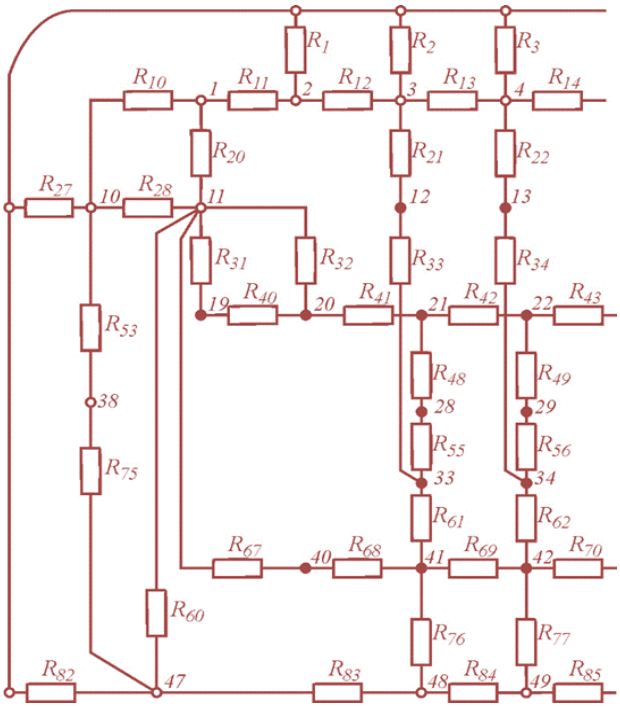

(b)

Figure 3. Sketch (a) and a fragment of the equivalent thermal circuit of induction motor: 1–10, 18 denote frame, 11, 17 denote internal air, 12–16 denote stator yoke, 19, 20, 26, 27 denote end parts of stator winding, 21–25 denote slot part of stator winding, 28–32 denote upper par of the stator teeth, 33–37 denote the lower part of stator teeth, 38–39 denote bears, 40, 46 denote end ring of rotoiw winding, 41–45 denote bars of rotor winding, 47–53 denote rotor shaft, black nodes denote the source of power losses (active nodes), hollow nodes denote passive units

The power loss in the motor active nodes is determined on the basis of the IM simulation using a T-shaped equivalent circuit of the motor with the rotor parameters brought to the parameters of the stator winding and replacing the motor mechanical load with alternating active resistance (Figure 4) (Lim & Nam, 2004; Kosmodamianskiy et al., 2015).

The main sources of IM losses are copper of the stator and rotor windings (rods and their rings), steel of the stator and rotor cores, as well as mechanical friction losses in the bearings. For the correct determination of losses in an equivalent IM circuit, it is necessary to take into account all-electric and magnetic losses. The greatest difficulty is accounting for steel losses.

The inclusion in the equivalent circuit of resistance parallel to mutual inductance, which is proportional to the losses in steel, is the best option for their modeling (Lim & Nam, 2004). With this approach, the distribution of losses in the rotor windings, stator steel, and stator windings is in the best agreement with the actual picture. Figure 2.13 shows an equivalent circuit of one motor phase for the case described above.

Figure 4 uses the following designations R_c, R_s, R_r - resistance, equivalent to losses in steel,

resistance of the stator and rotor windings (reduced to the stator winding); L_μ, $L_{\sigma s}$, $L_{\sigma r}$, - mutual inductance, dissipation inductance of the stator winding and rotor (reduced to the stator winding); I_s, I_c, I_r, I_μ, U_s –currents and voltage in the corresponding branches of the circuit.

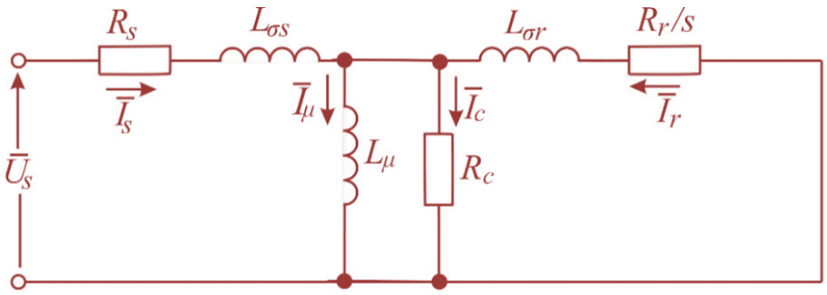

Figure 4: Equivalent circuit of one phase of the induction motor.

In order to consider the influence of eddy currents, it is possible to turn inductance in parallel with the R_c resistor. However, an analysis of the papers showed that the calculation accuracy will change insignificantly if this inductance is neglected (Aissa & Eddine, (2009).

The consideration of the nonlinearity of steel losses on frequency is determined by the dependence:

$$R_c = \begin{cases} 88.3135 + 5.646 f_s + 0.0534 f_s^2, & f_s \le 50Hz, \\ 1261.3 - 37868 / f_s, & f_s > 50Hz \end{cases}$$

Due to the fact that the effect of current displacement has a significant influence on an induction motor when it operates at lower frequencies, the resistance of the rotor winding must be determined with its consideration to obtain the most complete picture of energy and electromechanical processes. Accordingly, the expressions for determining active and inductive resistance will take the form:

$$R_r = K_R R_{гп} + R_{гл}, \quad X_r = K_X X_{гп} + X_{гл},$$

where $R_{гл}$ and $X_{гл}$ – resistance sections of short-circuit rings between adjacent rotor rods, $R_{гп}$ and $X_{гп}$ – resistance of the groove part of the rotor winding, K_R and K_X – coefficients that take into account changes in the active and inductive rotor resistances under the effect of current displacement:

$$K_R = \chi \frac{sh2\chi + \sin 2\chi}{ch2\chi - \cos 2\chi}, \quad K_X = \frac{3}{2\chi} \times \frac{sh2\chi - \sin 2\chi}{ch2\chi - \cos 2\chi},$$

where $\chi = 2\rho \times 10^{-3} \times h \times \sqrt{\frac{sf_1 b}{10 r b_п}}$ – reduced rod height, b – rod width, h - rod height, b_n - groove width, ρ - specific resistance of the rod material.

To study the effect of temperature on the distribution of power losses during the induction motor operation, we use the following temperature dependence of the active resistance of the windings:

$$R = R_{20}\left[1 + \alpha (T - T_{20})\right], \qquad (3)$$

where R_{20} – active resistance of the induction motor winding at a temperature of $T_{20} = 20$ °C,

*Corresponding author (A.A.Pugachev) Email: alexander-pugachev@rambler.ru Volume 11 No.3 ISSN 2228-9860 eISSN 1906-9642 CODEN: ITJEA8
Paper ID:11A03F http://TUENGR.COM/V11/11A03F.pdf DOI: 10.14456/ITJEMAST.2020.46

α – temperature coefficient of resistance,

T – current temperature of the winding.

In order to analyze the energy processes occurring in the motor, it is necessary to evaluate them according to the following expressions.

Losses in the stator winding of the motor, W

$$\Delta P_s = 3I_s^2 R_s.$$

Losses in the winding (rods) of the motor rotor, W

$$\Delta P_r = 3I_r^2 R_r.$$

Losses in the core of the motor stator, W

$$\Delta P_c = 3I_c^2 R_c.$$

The torque developed on the motor shaft, N·m

$$M = 2M_к \frac{\left(1 + \frac{R_s}{R_r}\right)}{\frac{s_к}{s} + \frac{s}{s_к} + 2s_к \frac{R_s}{R_r}}, \quad (4)$$

where M_c – the critical torque of the motor, N·m;

s – sliping;

s_k – critical sliping.

To study the dependence of loss power on the motor torque, we solve Expression (4) with respect to the motor slip using a computer.

$$s = -\frac{s_к\left(\sqrt{-(R_r + R_S s_к)\times(M - M_к)\times(MR_r + M_к R_r - MR_S s_к + M_к R_S s_к)}\right)}{MR_r} - \frac{M_к R_r}{MR_r} + \frac{MR_S s_к}{MR_r} - \frac{M_к R_S s_к}{MR_r}, \quad (5)$$

The resulting Expression (5) is substituted into the system of Equation (3) and its roots should be found.

The calculation of the main energy characteristics of an induction motor is performed for the motor in question in the Matlab software package.

AO-63-4 motor parameters: U_{snom} = 220 B; I_{1nom} = 27,4 A; $2p$ = 4; M_{nom} = 89 N·m, P_{nom} = 14 kW; n_{nom} = 1460 rpm; $f_{s,nom}$ = 50 Hz; $X_{\sigma s}$ = 0,73 Ohm; $X_{\sigma r,nom}$ = 1,68 Ohm; R_s = 0,34 Ohm; $R_{r,start}$ = 0,41 Ohm; $R_{r,nom}$ = 0,29 Ohm; $X_{\mu,nom}$ = 31 Ohm; R_c = 504 Ohm; $X_{\sigma r,start}$ = 0,73 Ohm, where $2p$ – the number of poles of the stator winding, P_{nom} – nominal motor power.

4. DIFFERENTIAL EQUATIONS OF THE THERMAL STATE OF THE MOTOR. DETERMINATION OF SPECIFIC HEAT CAPACITIES OF THE MOTOR ELEMENTS

Depending on the mode of operation, unsteady thermal processes (transient thermal processes) occur in all IMs in different volumes. They differ from stationary (steady-state) ones in that the temperature of heating of the elements of the IM structures varies with time, that is, the heating curves contain aperiodic (free) components. Non-stationary thermal conditions can be caused by the

induction motor start, change in supply voltage and frequency, voltage and frequency control, reversal of the motor, and changes in the load on the shaft.

During the development of the motor ETC, the task was to study dynamic thermal processes that can be simulated by introducing the heat capacity of the nodes in Equation (3). As a result, the general form of the differential thermal state equation for the *i-th* motor node, compiled on the basis of the nodal potentials method written in the Cauchy form takes the form

$$C_i \frac{\P q_i}{\P t} = P_i - \sum_{n=1}^{n} \frac{q_i - q_n}{R_{i,n}}, \qquad i = 1...n. \tag{6}$$

The heat capacity of the *i-th* element of the motor is calculated as follows

$$C_i = \sum_{j=1}^{l} m_l \times c_l, \tag{7}$$

where m_l – element mass, kg,

c_l – specific heat of the material the motor element is made of, J/kg K. The *l* index in Expression (7) indicates various materials the motor element is made of.

In most cases, the heat capacity of the motor elements is determined quite simply if the certificate data and geometric dimensions are known. However, the heat capacities of some motor nodes need comment. The stator winding heat capacity consists of heat capacities of copper and insulation. The insulation mass can be calculated based on the coefficient of free space in the stator groove and the area of its isolation. It is also assumed the cross-sectional area of the turns of the frontal part of the stator winding equals the cross-sectional area of the turns in the groove part. Figure 5 shows a fragment of the inclusion of the heat capacities of elements in the previously developed ETC of the motor.

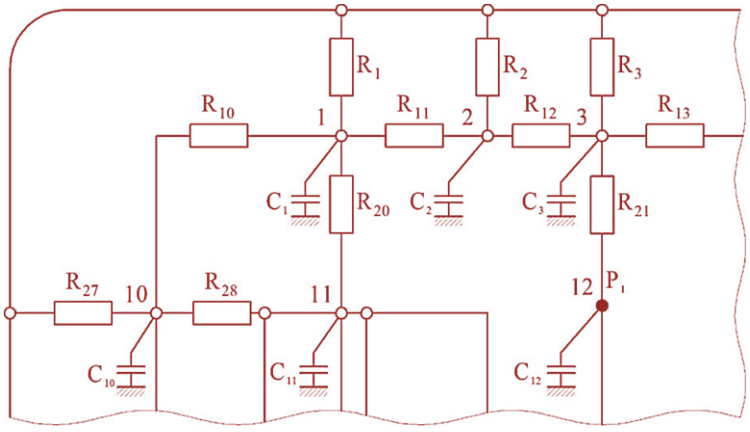

Figure 5: Fragment of a dynamic ETC.

For ETC units in non-stationary modes, we specify the masses used to determine their heat capacities: $m_1 \ldots m_9$ are the masses of the elementary parts of the motor block, m_{10} and m_{18} are the masses of the left and right end caps of the motor block, $m_{12} \ldots m_{16}$ are the masses of the elementary parts of the core stator, $m_{19} \ldots m_{27}$ - masses of elementary segments of the stator winding, $m_{28} \ldots m_{37}$ - masses of elementary segments of stator teeth, m_{38} and m_{39} - masses of motor bearings, $m_{40} \ldots m_{46}$ - masses of elementary segments of the rotor winding, $m_{47} \ldots m_{53}$ - masses of elementary parts of the rotor shaft.

The system of differential equations of thermal state for 53 engine nodes takes the form

*Corresponding author (A.A.Pugachev) Email: alexander-pugachev@rambler.ru Volume 11 No.3 ISSN 2228-9860 eISSN 1906-9642 CODEN: ITJEA8
Paper ID:11A03F http://TUENGR.COM/V11/11A03F.pdf DOI: 10.14456/ITJEMAST.2020.46

according to Expression (6).

5. SIMULATION RESULTS

The developed dynamic ETC of the motor in question was used to simulate thermal processes at various values of the supply current of 0.8 I_{nom}, 0.9 I_{nom} and 1.0 I_{nom}. The system of differential equations consisting of Equation (6) was solved by the Taylor method.

Figures 6-9 show the heating curves of the motor components for four cross-sections, obtained as a result of modeling in Matlab Simulink, with a supply current of 0.8 I_{nom}. To study the motor thermal state, the following units were selected: 1 - stator winding, 2 - rotor winding (rods), 3 - core with rotor shaft, 4 - upper part of stator teeth, 5 - the lower part of teeth, 6 - stator core and 7 - motor housing. The time of the transitional heating process is taken to be 12000 s or 200 minutes.

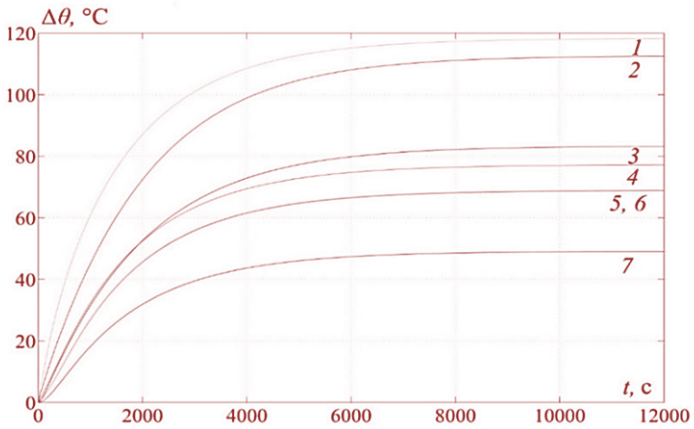

Figure 6: Heating curves of the motor components in a cross-section passing through the frontal part of the stator winding from the cooling air supply side.

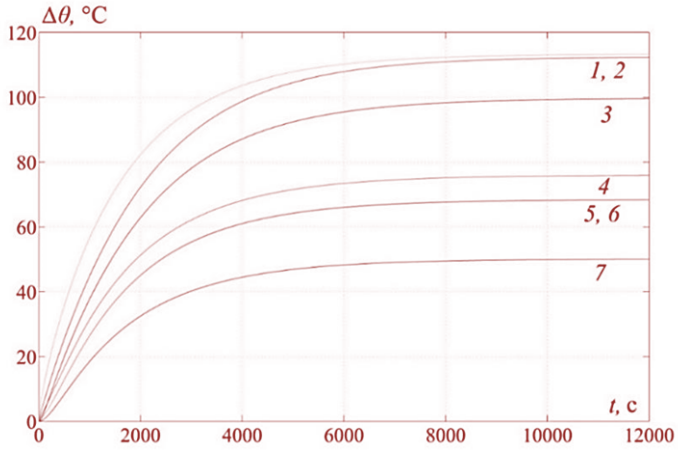

Figure 7: Heating curves of the motor components in the middle cross-section.

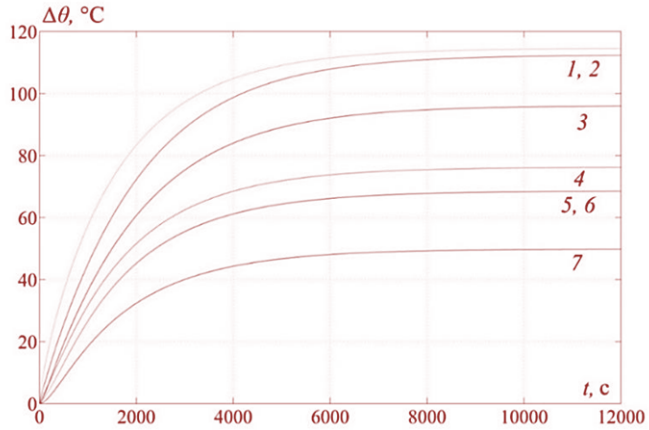

Figure 8: Heating curves of the motor components in the transverse cross-section at a distance of 2/3 of the stator winding from the cooling air supply side

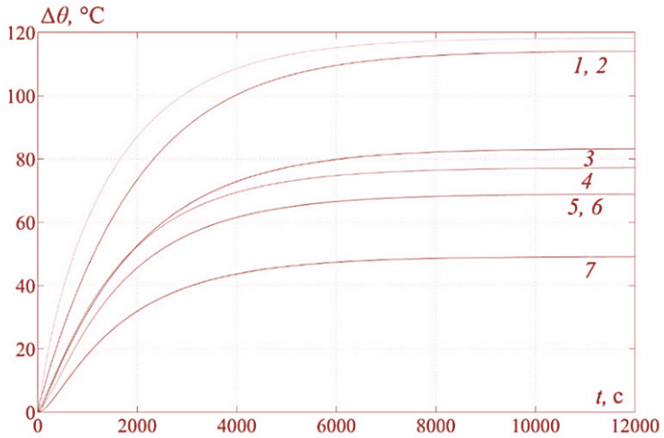

Figure 9: Heating curves of the motor components in the transverse section passing through the frontal part of the stator winding opposite to the cooling air supply side.

The resulting cooling curves of the motor components with a supply of cooling air equal to G_{air} = 0.95 m^3 / s and a stator current TAD equal to 0.8 I_{nom} are shown in Figures 10-13. The transitional process of cooling the motor was 9000 s or 150 min.

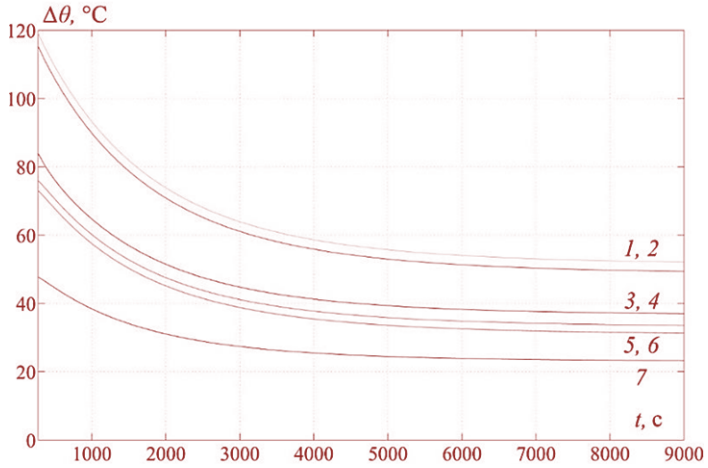

Figure 10: Cooling curves of motor components in a cross-section passing through the frontal part of the stator winding from the cooling air supply side.

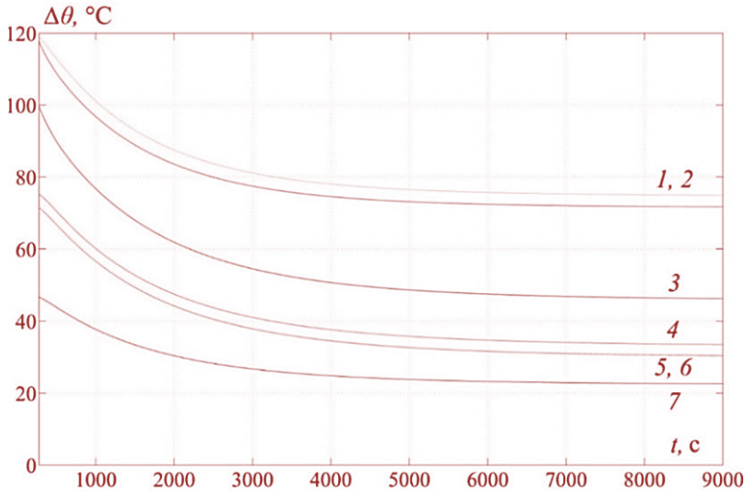

Figure 11: Cooling curves of motor components in the middle cross-section.

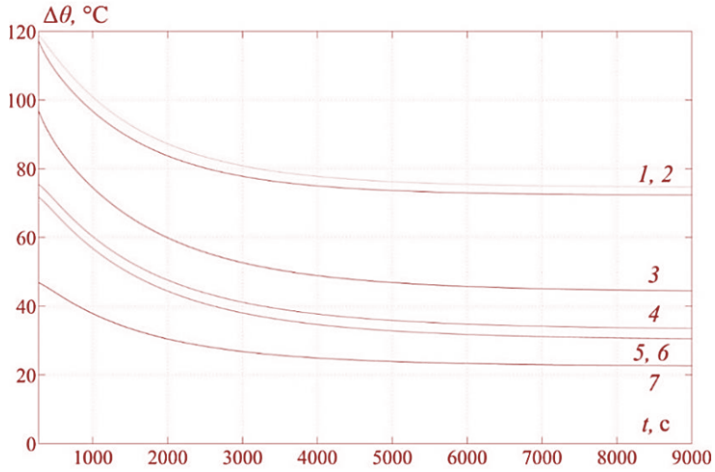

Figure 12: Cooling curves of motor components in the transverse cross-section at a distance of 2/3 of the stator winding on the cooling air supply side.

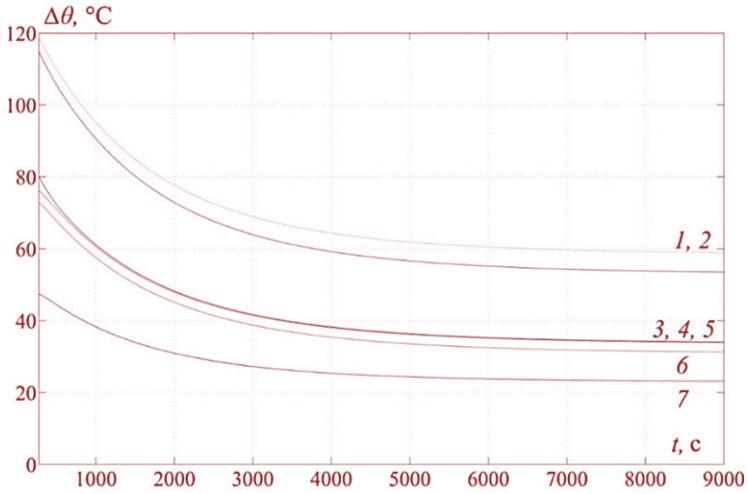

Figure 13: Cooling curves of motor components in the transverse cross-section passing through the frontal part of the stator winding from the opposite side of the cooling air supply.

In the process of studying the thermal state of the motor, the temperature excess distributions along the length of the stator and rotor were considered and are shown in Figures 14 - 16. The curves were plotted at nine and five points respectively for the stator and rotor using the third-order Lagrange interpolation polynomial. The reference point along the abscissa is the point of cooling air entry.

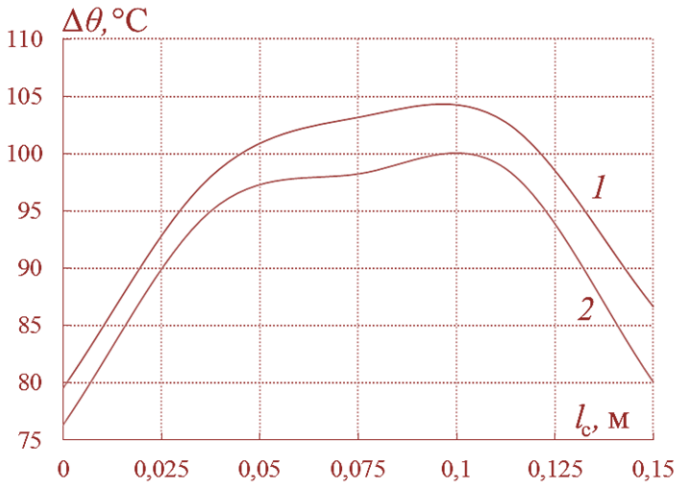

Figure 14: Temperature distribution along the length of the stator *1* and rotor *2* winding at $I_s = 0.8\ I_{nom}$.

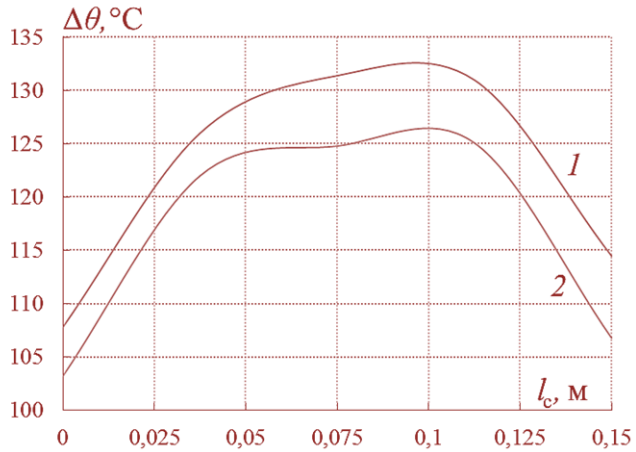

Figure 15: Temperature distribution along the length of the stator *1* and rotor *2* winding at $I_s = 0.9\ I_{nom}$

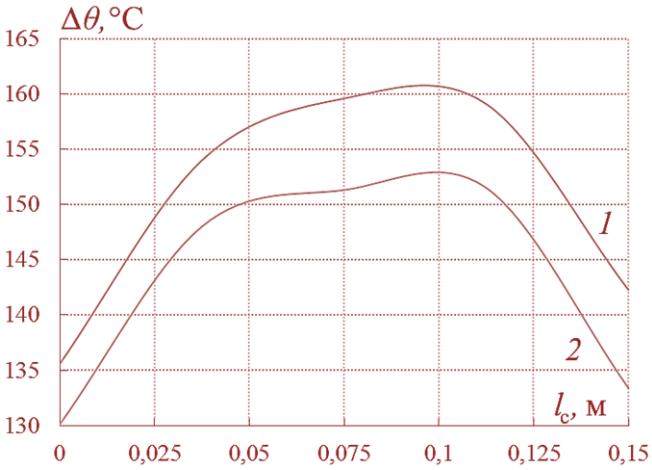

Figure 16: Temperature distribution along the length of the stator *1* and rotor *2* winding at $I_s = 1.0\ I_{nom}$

6. DISCUSSION

The analysis of the results shown in Figures 6-9 allows us to conclude that the most heated motor components in the absence of cooling are the stator and rotor windings in the middle section. The temperature of the stator winding is on average 5°C higher than the temperature of the rotor winding along the entire length of the motor. The least heated motor assembly is the motor housing.

*Corresponding author (A.A.Pugachev) Email: alexander-pugachev@rambler.ru Volume 11 No.3 ISSN 2228-9860 eISSN 1906-9642 CODEN: ITJEA8
Paper ID:11A03F http://TUENGR.COM/V11/11A03F.pdf DOI: 10.14456/ITJEMAST.2020.46

As the results in Figures 10–13 demonstrate, the most heat-loaded motor component when using cooling is the groove part of the stator winding at a distance of 2/3 of its length on the cooling air supply side. The next largest heating motor component is the winding (rods) of the rotor.

According to the results in Figures 14-16, the temperature distribution along the length of the stator and rotor windings is in the form of an asymmetric bell. At the same time, a larger temperature difference between the stator winding and the rotor, which reaches 10°C, corresponds to a larger I_s value of the stator current.

The results obtained confirm that the more intense the induction motor mode of operation, i.e. the greater the stator current and the more intense heat generation, the more different are the temperatures of adjacent parts of the electric machine.

The analysis of the results indicates that the stator winding of the induction motor experiences the greatest overheating. This is because, unlike the rotor, the stator does not have ventilation ducts and blades for forced cooling. Therefore, in the synthesis of cooling systems or automatic temperature control systems, all considerations regarding the IM temperature must be attributed to the stator winding as a temperature-limiting component.

The application of the developed model allows us, in addition to determining local temperatures at individual points of the motor, to find the average temperature values of the stator and rotor windings to correct the value of the current resistance of the windings, which is critical for closed-loop vector control systems and direct torque control.

The use of simulation modeling is fraught with obvious difficulties associated with the fact that the exact determination of the thermal circuit parameters is difficult because it requires too much information, both theoretical and experimental studies of a particular type of motor. In addition, some parameters change directly during operation, depending on the speed and temperature of the cooling air, humidity, etc. All of these factors can introduce errors in temperature determination.

At the same time, the proposed approach has an absolute advantage over the indirect determination of the average temperature by taking into account changes in the stator winding resistance, since in the latter case, satisfactory accuracy is ensured either only in the low-frequency mode of the stator current, at which the voltage drop across the stator active resistance is comparable with the ETC induced by the stator winding, or by introducing an additional component into the voltage supplied to the stator winding (Kosmodamianskii & Pugachev, 2018), which is difficult to implement in electric drives with vector control, where the task for the stator voltage is determined by the settings of the regulators of closed current loops. An additional component is considered by regulators as a disturbance, which, depending on the settings, they seek to minimize or completely eliminate. The resulting calculation accuracy is comparable to the accuracy provided by the ETC use.

Thus, the use of behavioral modeling to assess the temperature distribution over the internal volume of an induction motor and the average temperatures of the stator and rotor windings is a competitive option and its accuracy depends on the completeness and reliability of the initial data on the design, size and materials of the induction motor, and the performance depends on the hardware support of calculations.

7. CONCLUSION

The analysis of the heating and cooling processes of induction motors showed that the steady and unsteady thermal state of an induction motor directly depends on the design features, geometric dimensions, as well as the cooling method used. The accuracy of mathematical calculations is

determined by the correctness of the source data. Therefore, the results of calculations of thermal models for different motors will give different results, and not only in quantitative but also in qualitative terms. Therefore, confirmation of the adequacy of the developed mathematical model of thermal processes in an electric machine based on data obtained in other papers will be incorrect and unreliable. Thus, to predict the induction motor thermal state during its operation, it is necessary to develop its own mathematical model for a specific type of electric motor. Checking the adequacy of the mathematical model should be carried out according to the data obtained during experimental tests on the investigated motor, or its physical model.

In this work, to study the thermal state of the motor, the ETC method is adopted. A mathematical model has been developed for studying steady and transient thermal processes of the induction motor, consisting of fifty-three nodes, thirty-one of which are active sources of heat. As a result of the behavioral modeling of the IM ETC, it was found that the groove part of the stator winding experiences the greatest overheating at a distance of 2/3 from the cooling air inlet, the next largest heating component is the rotor winding (rods) from the side opposite to the cooling air supply; the difference in temperature between the groove part of the stator winding and the rotor rods can reach 2-10°C, the transition process for all IM nodes is approximately the same and differs by no more than 5-10%. The reliability of the results is confirmed by the results of the experimental studies.

The application of the developed model allows us to determine both local temperatures in individual motor nodes and average values of the temperature of the motor windings, which is why behavioral modeling based on ETCs can be recommended for use not only in cooling systems (automatic temperature control) but in control systems of electric drives as well.

8. AVAILABILITY OF DATA AND MATERIAL

Information used and generated from this work is available by contacting the corresponding author.

9. ACKNOWLEDGMENT

This work was financially supported by the Ministry of Education and Science of the Russian Federation (project No. 8.1729.2017/4.6).

10. REFERENCES

Aissa, K., & Eddine, K. D. (2009). Vector control using series iron loss model of induction motors and power loss minimization. *World Academy of Science, Engineering and Technology*, *52*, 142-148.

Briz, F., Degner, M. W., Guerrero, J. M., & Diez, A. B. (2008). Temperature estimation in inverter-fed machines using high-frequency carrier signal injection. *IEEE Transactions on Industry Applications*, *44*(3), 799-808.

Champenois, G., Roye, D., & Zhu, D. S. (1994). Electrical and thermal performance predictions in inverter-fed squirrel-cage induction motor drives. *Electric machines and power systems*, *22*(3), 355-369.

Huai, Y., Melnik, R. V., & Thogersen, P. B. (2003). Computational analysis of temperature rise phenomena in electric induction motors. *Applied Thermal Engineering*, *23*(7), 779-795.

Kosmodamianskii, A. S., & Pugachev, A. A. (2018). Modeling of Sensorless Determination of the Resistance and Temperature of the Stator and Rotor Windings of an Asynchronous Motor. *Russian Electrical Engineering*, *89*(9), 512-517.

*Corresponding author (A.A.Pugachev) Email: alexander-pugachev@rambler.ru Volume 11 No.3 ISSN 2228-9860 eISSN 1906-9642 CODEN: ITJEA8
Paper ID:11A03F http://TUENGR.COM/V11/11A03F.pdf DOI: 10.14456/ITJEMAST.2020.46

Kosmodamianskii, A. S., Vorob'ev, V. I., & Pugachev, A. A. (2012). Induction motor drives with minimal power losses. *Russian Electrical Engineering*, *83*(12), 667-671.

Kosmodamianskii, A. S., Vorob'ev, V. I., & Pugachev, A. A. (2015). Direct torque control of induction motors fed by a single frequency converter. *Russian Electrical Engineering*, *86*(9), 527-533.

Kosmodamianskii, A. S., Vorobiev, V. I., & Pugachev, A. A. (2011). The temperature effect on the performance of a traction asynchronous motor. *Russian Electrical Engineering*, *82*(8), 445.

Kosmodamianskiy, A. S., Vorobiev, V. I., & Pugachev, A. A. (2015). Automatic temperature regulation system of locomotive traction induction motors with power losses minimization. *JITA-JOURNAL OF INFORMATION TECHNOLOGY AND APLICATIONS*, *9*(1).

Krishnan, V. (2001). *Electric Motor Drives: modeling, analysis and control*. Virginia Tech, Blacksburg, VA.

Kylander, G. (1995). *Thermal modelling of small cage induction motors*. Chalmers University of Technology.

Lim, S., & Nam, K. (2004). Loss-minimising control scheme for induction motors. *IEE Proceedings-Electric Power Applications*, *151*(4), 385-397.

Mahdavi, S., Herold, T., & Hameyer, K. (2013, October). Thermal modeling as a tool to determine the overload capability of electrical machines. In *2013 International Conference on Electrical Machines and Systems (ICEMS)* (pp. 454-458). IEEE.

Mellor, P. H., Roberts, D., & Turner, D. R. (1991, September). Lumped parameter thermal model for electrical machines of TEFC design. In *IEE Proceedings B (Electric Power Applications)* (Vol. 138, No. 5, pp. 205-218). IET Digital Library.

Mezani, S., Takorabet, N., & Laporte, B. (2005). A combined electromagnetic and thermal analysis of induction motors. *IEEE transactions on Magnetics*, *41*(5), 1572-1575.

Motor Reliability Working Group. (1985). Report of large motor reliability survey of industrial and commercial installations, Part I. *IEEE Trans. Industrial Applications*, *1*(4), 865-872.

Novotny, D. W., & Lipo, T. A. (1996). *Vector control and dynamics of AC drives* (Vol. 1). Oxford university press.

Pugachev, A. A., & Kosmodamianskii, A. S. (2017). A simplified equivalent thermal circuit for the substitution of a stator in an induction motor. *Russian Electrical Engineering*, *88*(9), 600-604.

Staton, D. A. (2001, June). Thermal computer aided design-advancing the revolution in compact motors. In *IEMDC 2001. IEEE International Electric Machines and Drives Conference (Cat. No. 01EX485)* (pp. 858-863). IEEE.

Staton, D. A., & Cavagnino, A. (2008). Convection heat transfer and flow calculations suitable for electric machines thermal models. *IEEE transactions on industrial electronics*, *55*(10), 3509-3516.

Trigeol, J. F., Bertin, Y., & Lagonotte, P. (2006). Thermal modeling of an induction machine through the association of two numerical approaches. *IEEE Transactions on Energy Conversion*, *21*(2), 314-323.

Dr.A.A. Pugachev is an Associate Professor of Bryansk State Technical University. He got a Ph.D. degree. His Orcid ID is orcid.org/0000-0002-1836-0923.

Dr.A.Yu. Drakin is an Associate Professor of Bryansk State Technical University. He got a Ph.D. degree. His Orcid ID is orcid.org/0000-0001-5315-3834.

A.N. Shkolin is a Researcher of Bryansk State Technical University, Russia. His Orcid ID is orcid.org/0000-0001-5210-1370.